A FRAMEWORK FOR UNCERTAINTY QUANTIFICATION IN NONLINEAR MULTI-BODY SYSTEM DYNAMICS

D. Negrut* and M. Datar
Department of Mechanical Engineering
University of Wisconsin
Madison, WI

D. Gorsich and D. Lamb
U.S. Army Tank-Automotive Research Development and Engineering Center
Warren, MI

ABSTRACT

This paper outlines a methodology for determining the statistics associated with the time evolution of a nonlinear multi-body dynamic system operated under input uncertainty. The focus is on the dynamics of ground vehicle systems in environments characterized by multiple sources of uncertainty: road topography, friction coefficient at the road/tire interface and aerodynamic force loading. Drawing on parametric maximum likelihood estimation, the methodology outlined is general and can be applied to systematically study the impact of sources of uncertainty characterized herein by random processes. The proposed framework is demonstrated through a study that characterizes the uncertainty induced in the loading of the lower control arm of an SUV type vehicle by uncertainty associated with road topography.

1. INTRODUCTION

The goal of this work is to establish an analytically sound and computationally efficient framework for quantifying uncertainty in the dynamics of complex multi-body systems. The *motivating question* for this effort is as follows: how can one predict an average response and produce a confidence interval in relation to the time evolution of a complex multi-body system given a certain degree of input uncertainty? Herein, of interest is answering this question for *ground vehicle systems* whose dynamics are obtained as the solution of a set of differential-algebraic equations (Hairer; Wanner 1996). The differential equations follow from Newton's second law. The algebraic equations are nonlinear kinematic equations that constrain the evolution of the bodies that make up the system (Haug 1989).

The motivating question above is relevant for vehicle Condition-Based Maintenance (CBM) where the goal is to predict durability and fatigue of system components. The statistics of lower control arm loading in a High-Mobility Multi-Wheeled Vehicle (HMMWV) obtained through a multi-body dynamics simulation become the input to a durability analysis that can predict in a stochastic framework the condition of the part and recommend or postpone system maintenance. A stochastic characterization of system dynamics is also of interest in understanding the limit behavior of a dynamic system. For instance, providing real-time confidence intervals for certain vehicle maneuvers are useful in assessing its control when operating in icy road conditions.

Vehicle dynamics analysis under uncertain environment conditions, e.g. road profile (elevation, roughness, friction coefficient) and aerodynamic loading, requires approaches that draw on random functions. The methodology is substantially more involved than required for handling uncertainty that enters the dynamic response through discrete design parameters associated with the model. For instance, uncertainty in suspension spring stiffness or damping rates can be handled through random variables. In this case, methods such as the polynomial chaos (PC), see, for instance, (Xiu; Karniadakis 2002) are suitable provided the number of random variables is small. This approach is not suitable here since a discretization of the road leads to a very large number of random variables (the road attributes at each road grid point). Moreover, the PC methodology requires direct access and modification of the computer program used to run the deterministic simulation of the dynamic system to produce first and second order moment statistical information. This represents a serious limitation if relying on commercial off-the-shelf (COTS) software, which is most often the case in industry when running complex high-fidelity vehicle dynamics simulation.

In conjunction with Monte Carlo analysis, the alternative considered herein relies on random functions to capture uncertainty in system parameters and/or input. Limiting the discussion to three-dimensional road profiles, the methodology samples a posterior distribution that is conditioned on available road profile measurements. Two paths can be followed to implement this methodology. The first draws on a parametric representation of the uncertainty; the second is nonparametric in nature and as

Report Documentation Page

Form Approved
OMB No. 0704-0188

1. REPORT DATE	2. REPORT TYPE	3. DATES COVERED
22 SEP 2008	**N/A**	**-**

4. TITLE AND SUBTITLE **A Framework for Uncertainty Quantification in Nonlinear Multi-body System Dynamics**	5a. CONTRACT NUMBER 5b. GRANT NUMBER 5c. PROGRAM ELEMENT NUMBER
6. AUTHOR(S) **David Gorsich; David Lamb; M. Datar; D. Negrut**	5d. PROJECT NUMBER 5e. TASK NUMBER 5f. WORK UNIT NUMBER
7. PERFORMING ORGANIZATION NAME(S) AND ADDRESS(ES) **US Army RDECOM-TARDEC 6501 E 11 Mile Rd Warren, MI 48397-5000**	8. PERFORMING ORGANIZATION REPORT NUMBER **19170RC**
9. SPONSORING/MONITORING AGENCY NAME(S) AND ADDRESS(ES)	10. SPONSOR/MONITOR'S ACRONYM(S) **TACOM/TARDEC** 11. SPONSOR/MONITOR'S REPORT NUMBER(S) **19170RC**

12. DISTRIBUTION/AVAILABILITY STATEMENT
Approved for public release, distribution unlimited

13. SUPPLEMENTARY NOTES
Presented at the 26th Army Science Conference, 1-4 December 2008, Orlando, Florida, United States, The original document contains color images.

14. ABSTRACT

15. SUBJECT TERMS

16. SECURITY CLASSIFICATION OF:			17. LIMITATION OF ABSTRACT	18. NUMBER OF PAGES	19a. NAME OF RESPONSIBLE PERSON
a. REPORT	b. ABSTRACT	c. THIS PAGE			
unclassified	**unclassified**	**unclassified**	**SAR**	**8**	

Standard Form 298 (Rev. 8-98)
Prescribed by ANSI Std Z39-18

such is more expensive to implement. It can rely on smoothing techniques for kernel estimation such as Nadaraya-Watson estimation, see, for instance, (Wasserman 2006), or draw on the orthogonal discretization of the spectral representation of positive definite functions as suggested, for instance, by Genton and Gorsich (2002). The parametric approach is used in this paper by considering Gaussian Random Functions as priors for the road profiles. Furthermore, the discussion will be limited to stationary processes although undergoing research is also investigating the nonstationary case.

As is always the case, the use of a parametric model raises two legitimate questions: why a particular parametric model, and why is it fit to capture the statistics of the problem. Gaussian Random Functions (GRF) are completely defined by their correlation function, also known as variogram (Adler 1990; Cramér; Leadbetter 1967). Consequently, scrutinizing the choice of a parametric GRF model translates into scrutinizing the choice of correlation function. There are several families of correlation functions, the more common being exponential, Matérn, linear, spherical, and cubic (see, for instance Santner et al. (2003)). In this context, and in order to demonstrate the proposed framework for uncertainty quantification in multi-body dynamics, a representative problem will be investigated in conjunction with the selection of a GRF-based prior. Specifically, an analysis will be carried out to assess the sensitivity of the response of a vehicle to uncertainty in system input, here a road profile. Of interest is the load history for the lower-control arm of an HMMWV, a key quantity in the CBM of the vehicle. The parametric priors considered are (*i*) a GRF with a squared exponential correlation function, and (*ii*) the Ornstein-Uhlenbeck process. Pronounced sensitivity of the statistics of the loads acting on the lower control arm with respect to the choice of parametric model would suggest that serious consideration needs to be given to the nonparametric route, where the empirical step of variogram selection is avoided at the price of a more complex method and increase in simulation time.

2. UNCERTAINTY HANDLING METHODOLOGY

The discussion herein concerns handling uncertainty in spatial data. This situation commonly arises when limited information is used to generate road profiles subsequently used in the dynamic analysis of a ground vehicle. The uncertainty handling in aerodynamic loads, which can be addressed similarly, is not of primary interest in this study and will be omitted.

The uncertainty quantification framework proposed is described in Figure 1. The assumption is that learning data is available as the result of field measurements.

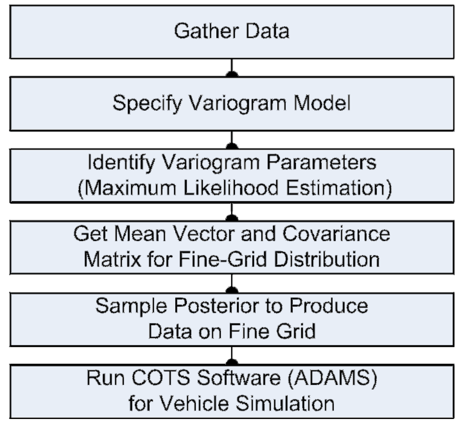

Figure 1: Proposed uncertainty quantification framework

Referring to Figure 2, the measured data is provided on a "coarse" measurement grid: at each (x_1, x_2) location an elevation y is available. From an uncertainty characterization perspective, the dimension of this problem is $d = 2$. For dynamic analysis, road information is ideally available everywhere on the road as a continuous data. As this is not possible, data is provided on a fine grid (right image in Figure 2). If working with a parametric model, a correlation function is selected and a learning stage follows. Its outcome, a set of hyper-parameters associated with the correlation function, is instrumental in generating the mean and covariance matrix ready to be used to generate sample road surfaces on the user specified fine grid.

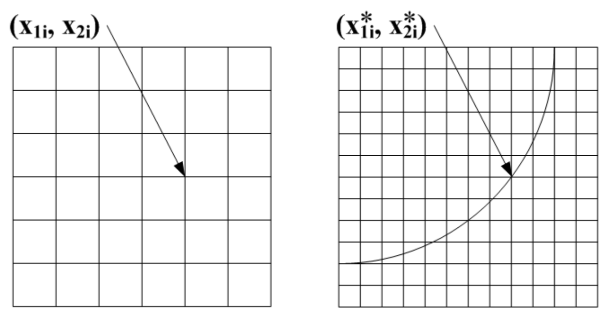

Figure 2. Coarse grid for learning, and fine grid employed in sampling for Monte Carlo analysis. Here $d = 2$.

Gaussian Random Functions (GRF) or processes lead to a very versatile approach for the simulation of infinite dimensional uncertainty. By definition, a spatially distributed random function $y(\mathbf{x})$, $\mathbf{x} \in \mathbb{R}^d$, is a GRF with mean function $m(\mathbf{x};\theta_1)$ and correlation function $k(\mathbf{x},\mathbf{x}';\theta_2)$ for any set of space points $\mathbf{X} = \{\mathbf{x}_1, \mathbf{x}_2, \ldots, \mathbf{x}_M\}$,

$$\mathbf{y}(\mathbf{X})=\begin{pmatrix} y_1 \\ y_2 \\ \vdots \\ y_M \end{pmatrix} \sim N\left(\mathbf{m}(\mathbf{X};\theta_1),\mathbf{K}(\mathbf{X},\mathbf{X};\theta_2)\right). \quad (1)$$

Here $y_i = y(\mathbf{x}_i)$, $\mathbf{m}\in\mathbb{R}^M$, $\mathbf{K}\in\mathbb{R}^{M\times M}$, and $N(\mathbf{m},\mathbf{K})$ is the M-variate normal distribution with mean $\mathbf{m}$ and covariance $\mathbf{K}$ given by

$$\mathbf{m}(\mathbf{X};\theta_1)=\begin{pmatrix} m(\mathbf{x}_1,\theta_1) \\ m(\mathbf{x}_2,\theta_1) \\ \vdots \\ m(\mathbf{x}_M,\theta_1) \end{pmatrix} \quad (2)$$

$$\mathbf{K}(\mathbf{X},\mathbf{X}';\theta_2)=\begin{pmatrix} k(x_1,x_1';\theta_2) & \cdots & k(x_1,x_N';\theta_2) \\ k(x_2,x_1';\theta_2) & \cdots & k(x_2,x_N';\theta_2) \\ \vdots & \vdots & \vdots \\ k(x_M,x_1';\theta_2) & \cdots & k(x_M,x_N';\theta_2) \end{pmatrix}, \quad (3)$$

where $\mathbf{X}'=\{\mathbf{x}_1',\mathbf{x}_2',\ldots,\mathbf{x}_N'\}$. The hyper-parameters θ_1 and θ_2 associated with the mean and covariance functions are obtained from a data set $\mathbf{y}(D)$ at nodes $D=\{d_1,\ldots,d_M\}$. The posterior distribution of the variable $\mathbf{y}(S)$ at node points $S=\{s_1,\ldots,s_N\}$, consistent with $\mathbf{y}(D)$, is $N(\mathbf{f}^*,\mathbf{K}^*)$ (Rasmussen; Williams 2006), where

$$\mathbf{f}^* = \mathbf{K}(S,D;\theta_2)\mathbf{K}^{-1}(D,D;\theta_2)\left(\mathbf{y}(D)-\mathbf{m}(D;\theta_1)\right)+\mathbf{m}(S;\theta_1)$$
$$\mathbf{K}^* = \mathbf{K}(S,S;\theta_2)-\mathbf{K}(S,D;\theta_2)\mathbf{K}^{-1}(D,D;\theta_2)\mathbf{K}(D,S;\theta_2)$$

The key issues in sampling from this posterior are a) how to obtain the hyper-parameters from data, and b) how to sample from $N(\mathbf{f}^*,\mathbf{K}^*)$, especially in the case where M is very large. The classical way to sample relies on a Cholesky factorization of $\mathbf{K}^*$, a costly order $O(M^3)$ operation. The efficient sampling question is discussed at length in (Schmitt et al. 2008a). A brief description of the hyper-parameter calculation follows.

2.1 Parameter Estimation

The method used herein for the estimation of the hyper-parameters data draws on maximum likelihood estimation (MLE) (Rasmussen; Williams 2006). Specifically, it selects those hyper-parameters that maximize the log-likelihood function associated with the measured data. In the multivariate Gaussian with mean $\mathbf{m}(\theta)\in\mathbb{R}^M$ and covariance matrix $\mathbf{K}(\theta)\in\mathbb{R}^{M\times M}$ case, the log-likelihood function assumes the form

$$\log p(\mathbf{y}\,|\,\theta) = -\frac{1}{2}\mathbf{W}^T\mathbf{K}(\theta)^{-1}\mathbf{W}-\frac{1}{2}\log|\mathbf{K}(\theta)|-\frac{M}{2}\log 2\pi$$

Here $\mathbf{W}=\mathbf{y}-\mathbf{m}(\theta)$ and $\mathbf{y}$ is the observed data. Note that $\theta=\{\theta_1,\theta_2\}$, and the dependence on the hyper-parameters θ appears by means of the coordinates $\mathbf{x}$. The gradients of the likelihood function can be computed analytically (Rasmussen; Williams 2006):

$$\frac{\partial}{\partial\theta_{1j}}\log p(\mathbf{y}\,|\,\theta) = -\left(\frac{\partial}{\partial\theta_{1j}}\mathbf{m}(\theta)\right)^T\mathbf{K}(\theta)^{-1}\mathbf{W}$$
$$\frac{\partial \log p(\mathbf{y}\,|\,\theta)}{\partial\theta_{2j}} = \frac{1}{2}\mathrm{tr}\left((\mathbf{K}(\theta)^{-1}\mathbf{W}(\mathbf{K}(\theta)^{-1}\mathbf{W})^T-\mathbf{K}(\theta)^{-1})\frac{\partial\mathbf{K}(\theta)}{\partial\theta_{2j}}\right)$$

MATLAB's *fsolve* function, which implements a quasi-Newton approach for nonlinear equations, was used to solve the first order optimality conditions $\frac{\partial \log p(\mathbf{y}\,|\,\theta)}{\partial\theta_{1j}}=0$ and $\frac{\partial \log p(\mathbf{y}\,|\,\theta)}{\partial\theta_{2j}}=0$ and determine the hyper-parameters θ_1 and θ_2. The entire approach hinges at this point upon the selection of the parametric mean and covariance function. It is common to select a zero mean prior $\mathbf{m}\equiv 0$, in which case only the θ_{2j} hyper-parameters associated with the covariance matrix remain to be inferred through MLE.

2.2 Covariance Function Selection

The parametric covariance function adopted determines the expression of the matrix $\mathbf{K}(\theta)$ of the previous subsection, and it requires an understanding of the underlying statistics associated with the data. In what follows, the discussion focuses on four common choices of correlation function: squared exponential (SE), Ornstein-Uhlenbeck (OU) (Uhlenbeck; Ornstein 1930), Matérn (Matérn 1960), and neural network (NN) (Neal 1996).

The SE correlation function assumes the form

$$k(\mathbf{x},\mathbf{x}';\theta_2)=\exp\left(-\left[\frac{(x_1-x_1')}{\theta_{21}}\right]^{2/\gamma}-\left[\frac{(x_2-x_2')}{\theta_{22}}\right]^{2/\gamma}\right), \quad (4)$$

where $\gamma=1$. The hyper-parameters θ_{21} and θ_{22} are called the characteristic lengths associated with the stochastic process and control the degree of spatial correlation. Large values of these coefficients lead to large correlation lengths, while small values reduce the spatial correlation leading in the limit to white noise, that is, completely uncorrelated data. The SE is the only continuously differentiable member of the family of exponential GRF. As such, it is not commonly used for capturing road profiles, which are typically not characterized by this level of smoothness. Rather, Stein

(Stein 1999) recommends the Matérn family with the correlation function

$$k(r;\theta_2) = \frac{2^{1-\nu}}{\Gamma(\nu)}\left(\frac{\sqrt{2\nu}r}{l}\right)^{\nu} K_{\nu}\left(\frac{\sqrt{2\nu}r}{l}\right), \quad (5)$$

where K_ν is the modified Bessel function and ν and l are positive hyper-parameters. The degree of smoothness of the ensuing GRF can be controlled through the parameter ν: the GRF is p-times differentiable if and only if $\nu > p$. Note that selecting $\gamma = 2$ in Eq. (4) leads to the OU random process, which is also a nonsmooth process although not as versatile as the Matérn family.

The three covariance models discussed so far: SE, OU, and Matérn are stationary. Referring to Eq. (1), this means that for any set of points $\mathbf{X} = \{\mathbf{x}_1, \mathbf{x}_2, \ldots, \mathbf{x}_M\}$, where M is arbitrary, and for any vector $\mathbf{h} \in \mathbb{R}^d$, $\mathbf{y}(\mathbf{X})$ and $\mathbf{y}(\mathbf{X}+\mathbf{h})$ always have the same mean and covariance matrix. In particular, when $M = 1$, this means that the GRF should have the same mean and variance everywhere. Clearly, the stationary assumption does not hold in many cases. For vehicle simulation, consider the case of a road with a pothole in it, which cannot be captured by stationary processes. A versatile nonstationary neural network covariance function has been proposed by Neal (1996):

$$k(\mathbf{x},\mathbf{x}';\Sigma) = \frac{2}{\pi}\sin^{-1}\left(\frac{2\tilde{\mathbf{x}}^T\Sigma\tilde{\mathbf{x}}'}{\sqrt{\left(1+2\tilde{\mathbf{x}}^T\Sigma\tilde{\mathbf{x}}\right)\left(1+2\tilde{\mathbf{x}}'^T\Sigma\tilde{\mathbf{x}}'\right)}}\right), \quad (6)$$

where $\tilde{\mathbf{x}} = (1, x_1, \ldots, x_d)^T$ is an augmented input vector; the symmetric positive definite matrix Σ contains the parameters associated with this GRF that are determined through MLE. Note that for the road profile problem $d = 2$.

Using this parameter estimation approach, a mean and co-variance function for Gaussian processes is determined. This is then used to generate new roads which are statistically equivalent to the road used in the learning process. Figure 5. shows the vehicle model in ADAMS/Car on two such roads.

3. NUMERICAL EXPERIMENT: PARAMETRIC MODEL SENSITIVITY

The numerical experiments carried out illustrate how the proposed uncertainty quantification framework is used to predict an average behavior and produce a confidence interval in relation to the time evolution of a nonlinear multi-body system. A high-fidelity vehicle model is considered and its time evolution is marked by uncertainty stemming from measurements of the road profile. This setup was chosen due to its relevance in CBM, where the interest is the statistics of the loads acting on the vehicle for durability analysis purposes. Note that a similar analysis is carried out for a simplified scenario that does not involve the MLE learning stage by Schmitt et al. (2008b) in conjunction with quantifying the uncertainty of vehicle dynamics when running on icy roads with a stochastic distribution of the tire/road friction coefficient.

3.1 Vehicle Model

The vehicle of interest in this work is a SUV-type vehicle similar to the Army's High Mobility Multi-Wheeled Vehicle (HMMWV). A high-fidelity model of the vehicle was generated in ADAMS, a widely used COTS software that contains a template library, ADAMS/Car, dedicated to ground vehicle modeling and simulation. The steering system is of rack-and-pinion type. The vehicle is equipped with an Ackerman type suspension system. The front and rear suspensions have the same topology but different link lengths. The location of the suspension subsystem is parameterized with respect to the chassis of the vehicle to allow for an easy editing of the assembly topology. Although not a topic of interest in this paper that deals with infinite dimensional stochastic processes, this parameterization of the suspension allows for a Monte-Carlo based approach to quantify the uncertainty in vehicle dynamics produced by this model subcomponent.

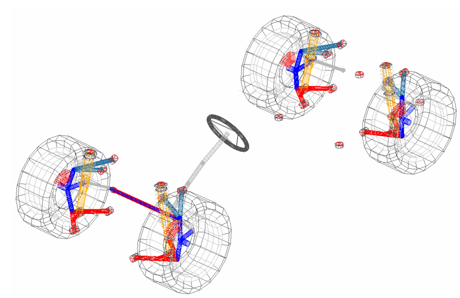

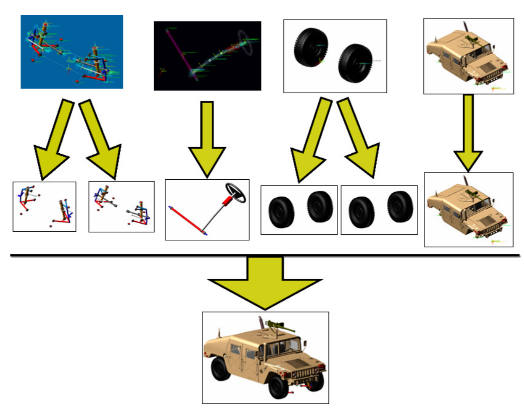

Figure 3. Up: Vehicle model, (no chassis geometry shown). Down: Schematic of how different subsystems are assembled to make a full vehicle model.

Figure 3 shows the topology of a vehicle with front and rear suspension, wheels, and steering subsystems. Different vehicle subsystems are individually modeled and are integrated together to form a full vehicle model. The chassis of the vehicle is modeled as a single component having appropriate mass-inertia properties. ADAMS/Flex is typically used to add compliance to the steering and/or chassis components of the vehicle. This process makes use of modal neutral format (MNF) files created using a third party finite element package such as ABAQUS.

3.2 Tire and Road Models

Two types of external forces act under normal conditions on the vehicle and influence its dynamics: forces at the tire-road interface and aerodynamic forces. Given the range of speeds at which the considered ground vehicle is driven, the former forces are prevalent and high-fidelity simulation depends critically on their accurate characterization. In this context, the SUV configuration of interest is designed to drive over a variety of terrains, from flat smooth pavement to off-road conditions.

In this study, the tire is modeled using a high-fidelity COTS software called FTire (Gipser 2005). FTire can be used for vehicle handling, ride comfort and durability studies on even or uneven roadways with extremely short obstacle wavelengths. It is a physics-based, highly nonlinear, dynamic tire model, which is fast (typically only 5 to 20 times slower than real-time) and numerically robust. The tire belt is described as an extensible and flexible ring carrying bending loads, elastically founded on the rim by distributed, partially dynamic stiffness in the radial, tangential, and lateral directions. The tire model is accurate at relatively high frequencies (up to 120 Hz) both in longitudinal and lateral directions. It works out of, and up to, a complete standstill without any additional computing effort or model switching. It is suitable for demanding applications such as ABS braking on uneven roadways.

The road models supported should accommodate the fidelity representation level required by the tire model considered. The road modeling environment of choice is the one provided by ADAMS, where the road is defined by a text based data file (rdf). This rdf file contains the information about road size, type (flat, periodic obstacles, stochastic 3D) and coefficients of friction over the road surface. Defining a flat road is trivial and an obstacle in the road (curb, roof-shaped) can be defined by specifying the size and shape of the obstacle. For roads with varying elevations in both lateral and longitudinal directions, a tessellated road definition is supported in ADAMS. The tessellated road is described by a set of vertices/nodes, which are grouped in sets of three to create a triangulated mesh that describes the entire road surface (see Figure 4). A coefficient of friction can be specified for each triangle. This road definition works well with both synthesized and measured road data and it was the solution embraced for the numerical results reported in this work.

The disadvantage of this road definition is that for each time step, the simulation has to check each triangle for contact with the tire patch leading to a major computational bottleneck (extremely long simulation times for large road profiles with high resolution). In order to simulate large road profiles, the regular grid road (rgr) file format can be used in conjunction with FTire. A conversion from tessellated to the new rgr format leads to smaller file sizes and significantly reduces CPU time per simulation step in that the CPU time required for the tire/terrain interaction is independent of the dimensions (length/width) of the road profile. This approach has been used in the past to analyze ride maneuvers that cover mile long distances.

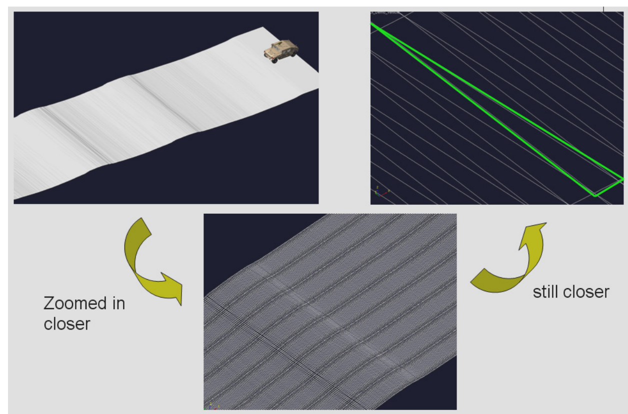

Figure 4: Road tessellation through a triangulation applied to a road profile

3.3 Numerical Results, Square Exponential

The SUV model discussed in subsection 3.1 was equipped with a set of four tires generated in the FTire modeling and simulation package discussed in subsection 3.2. The vehicle model was exercised through a straight-line maneuver over a road profile for which information is available on a grid as follows (see also Figure 4): in the x-direction, information is provided every 0.25 feet in 180 slices. In the y-direction, the data is provided at a distance of four feet apart in three slices. The length of the course in the x-direction was approximately 45 feet. The width of the road was 8 feet. Although not reported here, simulations up to one mile long have been run using this vehicle configuration.

The stochastic analysis proceeded according to the work flow in Figure 1. A road profile was provided and considered the outcome of a set of field measurements on a 180X3 grid as indicated above. MLE was carried out; the resulting characteristic lengths were $\theta_x = 4.5355$ and

$\theta_y = 0.8740$, which are identified in Eq. (4) with θ_{21} and θ_{22}, respectively. A set of 200 road profiles were generated by sampling of the posterior; Figure 5 illustrates two of them. The road profiles were relatively smooth in the sense that there was no road geometric feature of length comparable to the length of the tire/road contact patch. The terrain was considered rigid and with a constant friction coefficient.

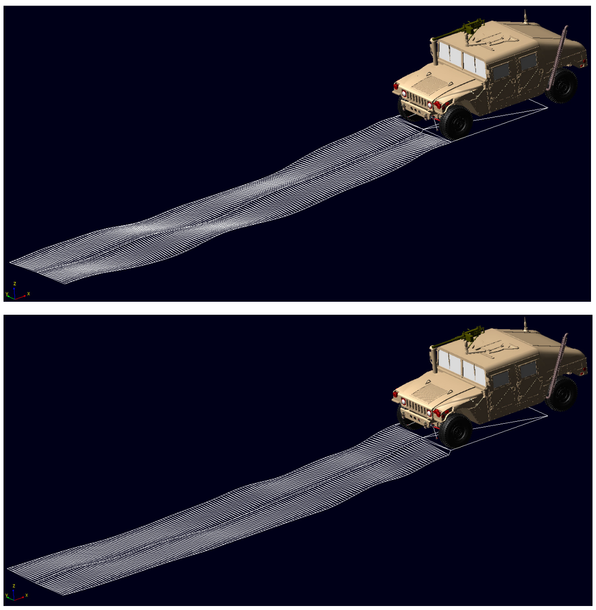

Figure 5. Vehicle on 2 different road surfaces. The two roads are generated using the same training data.

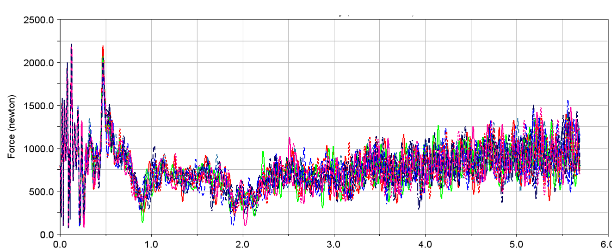

Figure 6. Vehicle response obtained using ADAMS. A subset of 10 out of the 200 simulations used to generate the statistics of the normal force response is displayed. The plot shows the reaction force in a suspension joint.

A batch of 200 ADAMS simulations were subsequently carried out to determine the statistics of the vehicle response. Ten responses are illustrated in Figure 6, which reports the reaction force in a suspension joint. Of interest here is the loading in the lower control arm (LCA) of the vehicle suspension, which is measured by the loads experienced by the suspension bushings connecting the LCA and the chassis. There are two such bushings, and there are two more connecting the upper control arm (UCA) to the chassis for a total of 16 bushing elements (eight UCA and eight LCA). Average behavior and a 95% confidence interval are provided for the LCA bushing load in Figure 7. Note that all results reported in the plots are in SI units.

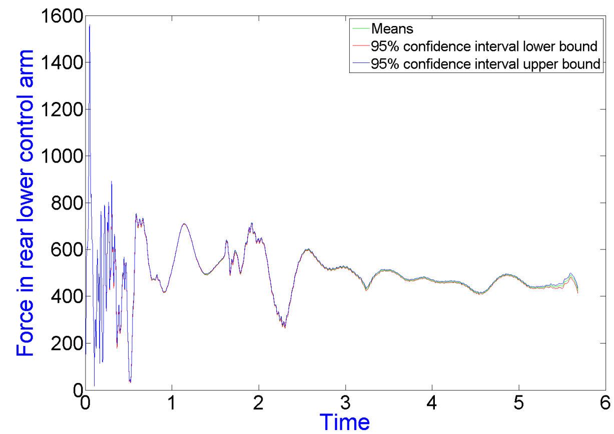

Figure 7. Statistics of vertical load, bushing attached to LCA.

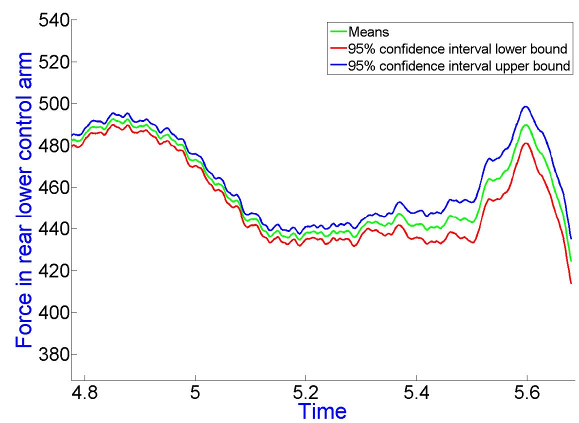

Figure 8. Statistics of vertical load, bushing attached to LCA. Detailed view focused on the last part of run.

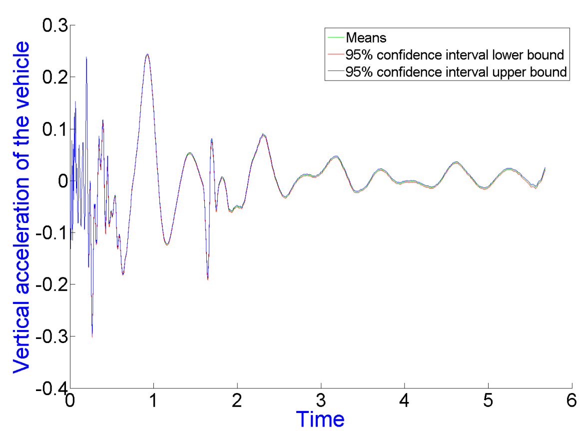

Figure 9. Statistics of vertical acceleration as measured at the CG position of the chassis: mean and 95% confidence interval.

3.4 Numerical Results, Ornstein-Uhlenbeck

The results reported in this subsection are obtained by setting $\gamma = 2$ in Eq. (4). This change leads to Ornstein-Uhlenbeck GRF posteriors that lack differentiability. In fact, the SE ($\gamma = 1$) is the only exponential GRF that is continuously differentiable. Figure 10 shows the load history for the same bushing element that was considered for the results in Figure 7. Figure 11 is a zoom-in to better gauge the 95% confidence interval for the LCA load. Finally, the vertical acceleration associated with the OU process is reported in Figure 12. Note that for OU the two characteristic lengths obtained at the end of the MLE stage are $\theta_x = 1.0849\text{e}+003$ and $\theta_y = 0.1830$.

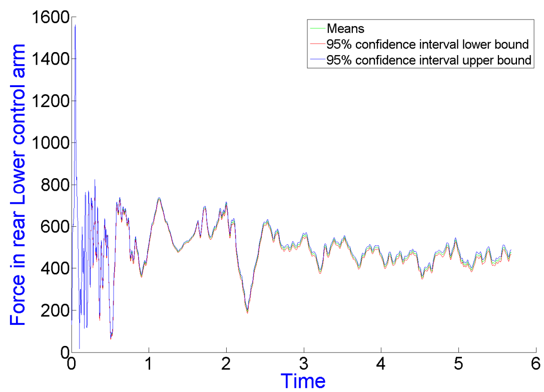

Figure 10. Vertical load statistics, bushing attached to LCA.

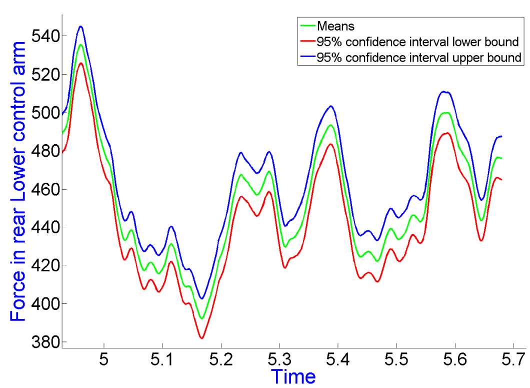

Figure 11. Statistics of vertical load, bushing attached to LCA. Detailed view focused on the last part of run.

3.5 Discussion of Numerical Results

The results reported in Figure 8 and Figure 11 suggest that the experimental data is gathered on a dense enough grid. Specifically, there is relatively small variance in the response of the vehicle, which is a very desirable response characteristic. This can be also seen in Figure 8, which illustrates the statistics associated with the last part of the simulation. This is an indication that the grid used is sufficiently fine to limit the amount of uncertainty stemming from the uncertainty in road profile. In other words, the measured road data is provided at a level of granularity sufficient to pinpoint with good precision the load history for the force acting at a hot point of the LCA.

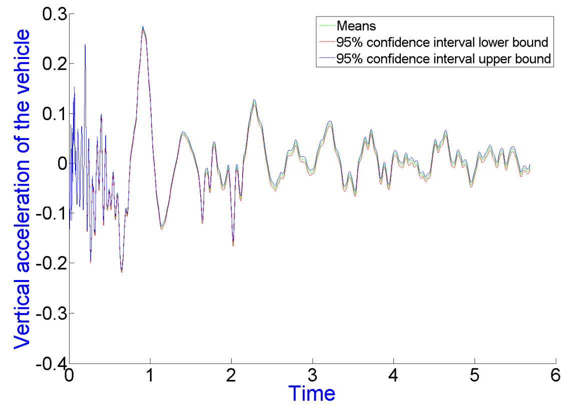

Figure 12. Statistics of vertical acceleration, as measured at the CG position of the chassis: mean and 95% confidence interval.

The results reported in Figure 9 indicate the statistics associated with the vertical acceleration of the center of gravity (CG) of the chassis. In this context, information regarding the vertical acceleration and the jerk measured at a location where the vehicle driver is positioned is valuable as it is used to gauge ride comfort and the potential for vibration induced fatigue during long term exposure of a vehicle driver.

Finally, the comparison of results reported in Figure 7 and Figure 10, or Figure 8 and Figure 11, or Figure 9 and Figure 12, demonstrates the qualitative difference between the SE and OU exponential GRFs. The OU family leads to processes that are nonsmooth, while the SE family leads to road profiles that are continuously differentiable. This is eventually reflected in the smoothness of the output: the SE response is smoother compared to the OU outcome. Nonetheless, there is good agreement between the results obtained with the OU and SE, and if this roughness associated with OU leads to any significant change in CBM decisions remains to be investigated. This task falls outside the scope of this study.

4. CONCLUSIONS AND FUTURE WORK

This paper outlines a methodology for determining the statistics associated with the time evolution of a nonlinear multi-body dynamic system operated under input uncertainty. The focus is on the dynamics of ground vehicle systems in environments characterized by multiple sources of uncertainty: road topography, friction coefficient at the road/tire interface and aerodynamic force loading. The methodology outlined is general and can be applied to systematically study the impact of sources of uncertainty that were characterized herein by random processes. The scope of the discussion is limited to the case of unknown road profiles at the wheel/road interface of an SUV. The same approach can be used in conjunction with vehicle design parameters by substituting the GRF machinery with that of sampling from a random variable distribution. The latter scenario is simpler and not discussed here. It would closely follow the methodology outlined in Figure 1 in the sense that one could deal with parametric or nonparametric models, and then invoke MLE to obtain the hyper-parameters associated with the posterior distribution. The latter is subsequently sampled in a Monte-Carlo analysis to gauge the impact of uncertainty on the dynamics of the model.

The results reported herein suggest that the choice of correlation function is important. Further work is needed to better understand the sensitivity of the system response with respect to the correlation function. In this context, two directions of future work could prove insightful. First, it would be useful to bring into the picture other GRF correlation functions, both stationary and non-stationary, to understand the importance of the parametric model choice. This direction is currently under investigation (Datar 2008). Second, it would be useful to lift the requirement that the stochastic approach be molded upon the GRF idea. Nonparametric models should be considered and the improved flexibility should be weighted against their more involved analytical derivation, method implementation, and computational burdens.

Even before considering nonparametric techniques the computational load associated with the methodology proposed can be significant. This is particularly the case when the amount of learning data is vast and/or the posterior is sampled on a very fine grid. This issue can be addressed by either allocating more computational power to solve the problem or by considering new sampling techniques. Recent inroads into better sampling techniques have been recently reported by Schmitt, Anitescu et al. (2008a), where a substantial reduction in sampling effort is demonstrated by the use of two new approaches. The first makes a periodicity assumption that enables a Fast Fourier Transform (FFT) technique to be used for posterior sampling, while the second uses compact kernel covariance functions to sample the posterior on small sliding windows that are continuously moved to follow the vehicle in its motion over the region of interest.

ACKNOWLEDGEMENT

D. Negrut would like to thank BAE Systems for providing partial financial support that allowed his participation in this research effort. M. Anitescu, K. Schmitt, J. Madsen, and N. Schafer are acknowledged for their valuable suggestions.

REFERENCES

Adler, R. J., 1990: *An Introduction to Continuity, Extrema, and Related Topics for General Gaussian Processes.* Institute of Mathematical Statistics.

Cramér, H., and M. R. Leadbetter, 1967: Stationary and related stochastic processes. Wiley

Datar, M., 2008: Uncertainty Quantification in Ground Vehicle Simulation, M.S. Thesis, Mechanical Engineering, University of Wisconsin-Madison.

Genton, M., and D. Gorsich, 2002: Nonparametric variogram and covariogram estimation with Fourier–Bessel matrices. Computational Statistics and Data Analysis, 41, 47-57.

Gipser, M., 2005: FTire: a physically based application-oriented tyre model for use with detailed MBS and finite-element suspension models. Vehicle Systems Dynamics, 43, 76 - 91.

Hairer, E., and G. Wanner, 1996: Solving Ordinary Differential Equations II: Stiff and Differential-Algebraic Problems. Second Revised ed. Vol. 14, Springer.

Haug, E. J., 1989: Computer-Aided Kinematics and Dynamics of Mechanical Systems. Volume I:Basic Methods. Allyn and Bacon.

Matérn, B., 1960: Spatial Variation (Lecture NotesStatist. 36). Springer, Berlin.

Neal, R., 1996: Bayesian Learning for Neural Networks. Springer.

Rasmussen, C. E., and C. K. I. Williams, 2006: Gaussian processes for machine learning. Springer.

Santner, T. J., B. J. Williams, and W. Notz, 2003: The Design and Analysis of Computer Experiments. Springer.

Schmitt, K., M. Anitescu, and D. Negrut, 2008a: Efficient sampling of dynamical systems with spatial uncertainty. International Journal for Numerical Methods in Engineering, submitted.

Schmitt, K., J. Madsen, M. Anitescu, and D. Negrut, 2008b: A Gaussian Process Based Approach for Handling Uncertainty in Vehicle Dynamics Simulations - IMECE2008-66664. 2008 ASME International Mechanical Engineering Congress and Exposition, Boston, MA, ASME.

Stein, M., 1999: Interpolation of Spatial Data: Some Theory for Kriging. Springer.

Uhlenbeck, G., and L. Ornstein, 1930: On the Theory of the Brownian Motion. Physical Review, 36, 823-841.

Wasserman, L., 2006: All of Nonparametric Statistics. Springer.

Xiu, D., and G. E. Karniadakis, 2002: The Wiener-Askey Polynomial Chaos for Stochastic Differential Equations. SIAM Journal on Scientific Computing, 24, 619-644.